

# Stability of highly shifted equilibria in a large aspect ratio low-field tokamak

P.-A. Gourdain,<sup>a)</sup> J.-N. Leboeuf, and R. Y. Neches

*Department of Physics and Astronomy, University of California, Los Angeles, Los Angeles, California 90095-1547, USA*

(Received 12 July 2007; accepted 18 October 2007; published online 26 November 2007)

In the long run, the economics of fusion will dictate that reactors confine large plasma pressure rather efficiently. A possible route manifests itself as equilibria with large shift of the plasma magnetic axis. This shift compresses the flux surfaces on the outer part of the plasma, hereby increasing the allowable plasma pressure a machine can confine for a given toroidal magnetic field, which is the main cost of the device. As a first step toward a reactor, we propose investigating the stability of such configurations in a low magnetic field high aspect ratio machine. By focusing our arguments solely on the shape of the toroidal plasma current density profile we discuss the stability of highly shifted equilibria and their robustness to current profile variations that could occur in actual experiments. The evolution of the plasma parameters, as the beta poloidal is increased, is also examined to give a better understanding of the difference in performance between the various regimes. © 2007 American Institute of Physics. [DOI: 10.1063/1.2807024]

## I. INTRODUCTION

The most promising candidate for a large-scale fusion reactor is the tokamak concept, where a closed magnetic configuration limits particle and heat losses, thereby avoiding excessive power input to maintain the appropriate plasma temperature. However, present day tokamaks only use the strong toroidal magnetic field, the main cost of the device, to confine particles as well as to improve stability. The weaker poloidal field, generated by the toroidal plasma current, participates solely in the equilibrium of pressure gradients. To quantify the pressure confinement efficiency the ratio of the kinetic pressure to the magnetic pressure is used,

$$\beta = 2\mu_0 \frac{p_{\text{axis}}}{B_{\text{axis}}^2} \text{ or } \langle \beta \rangle = 2\mu_0 \frac{\langle p \rangle}{\langle B^2 \rangle}. \quad (1)$$

The symbol  $\langle \cdot \rangle$  represents the volume average.  $p_{\text{axis}}$  is the plasma kinetic pressure at the magnetic axis, where the pressure is maximum and the poloidal field,  $B_p$ , is null.  $B_{\text{axis}}$  is the magnetic field on axis. In a finite aspect ratio tokamak,  $\langle \beta \rangle$  is typically below the 5% mark.

For the toroidal field to participate directly in the confinement of the pressure gradient, diamagnetic poloidal currents have to run in the plasma. They flow in the plane perpendicular to the toroidal (axisymmetric) direction. A measure of these currents is given by the poloidal beta,

$$\beta_p = 2\mu_0 \frac{\langle p \rangle}{\langle B_p^2 \rangle}. \quad (2)$$

If  $\beta_p \approx 1$ , the kinetic pressure is equilibrated only by the magnetic pressure of the poloidal field. In this case, the magnetic axis, where pressure is maximum, is found near the geometrical center of the plasma cross section (top set of

surfaces in Fig. 1). This configuration does not generate any diamagnetic poloidal currents. As  $\beta_p$  increases, the kinetic pressure becomes larger than the poloidal magnetic field pressure, as poloidal currents flow to equilibrate this excess of kinetic pressure. In largely diamagnetic plasmas, most of the pressure is confined solely by poloidal currents. Qualitatively, low and high  $\beta_p$  configurations differ in the arrangement of isopressure surfaces; as  $\beta_p$  increases, they are compressed on the low field side of the plasma (i.e., the outboard side of the device). This reorganization is called the Shafranov shift. Figure 1 characterizes low and high beta plasma discharges. All finite aspect ratio tokamaks are naturally stable at sufficiently low  $\beta_p$ .

However, large pressure gradient usually leads to plasma disruptions. A very simple criterion, the so-called Troyon limit,<sup>1</sup> uses the normal beta,

$$\beta_N = \frac{\langle \beta \rangle (\%) a (\text{m}) B_T (\text{T})}{I_p (\text{MA})}, \quad (3)$$

to characterize the ideal magnetohydrodynamics (MHD) stability properties of a given plasma. According to the Troyon limit, a plasma with a  $\beta_N$  above 3-4 will be unstable. This has lent credence to the fact that high  $\beta_p$  plasmas are inherently unstable. However recent research has not only demonstrated that high  $\beta_p$  equilibria exist<sup>2,3</sup> but that they can be robustly stable to many ideal MHD criteria.<sup>4</sup> To better understand the properties and stability of high  $\beta_p$  equilibria, a quantitative study of the most common ideal MHD criteria is undertaken in this paper. Since the range of plasma shapes and parameters is broad, we choose to limit this research to a low-field high-aspect-ratio device. Plasma shape (circular), magnetic field ( $B_T=0.25$  T) or toroidal function ( $F=1.25$  T m), major radius ( $R=5$  m), minor radius ( $a=1$  m), and total plasma current ( $I_p=50$  kA) were kept constant herein. They are the standard parameters of the Electric Tokamak.<sup>5</sup> The only free parameter in this study is the shape

<sup>a)</sup>Author to whom correspondence should be addressed. Electronic mail: gourdain@ucla.edu.

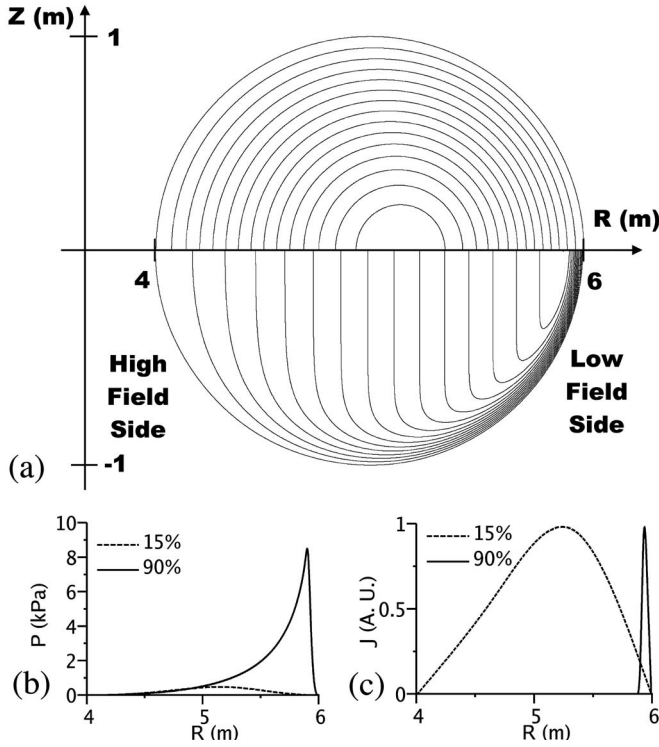


FIG. 1. (a) Flux surfaces for a circular plasma cross section. The  $Z$ -axis is the axis of axisymmetry (actually located at  $R=0$ ). Due to the up-down symmetry, only one half of the configurations is shown. The top set of surfaces is for a 15% Shafranov shift ( $\beta=1.8\%$ ,  $\beta_p=1.15$ ) and the lower set of surfaces represents an equilibrium with a 90% shift ( $\beta=35\%$ ,  $\beta_p=50$ ). The magnetic axis is located on the plane of symmetry ( $Z=0$ ) at  $R=5.15$  m (15% shift) and  $R=5.90$  m (90% shift). (b) Pressure and (c) normalized current density profiles for the same shifts.

of the toroidal current density profile. Mercier,<sup>6</sup> Glasser–Greene–Johnson (GGJ) resistive<sup>7</sup> and high- $n$  ideal ballooning criteria<sup>8</sup> as well as the energy of fixed and free boundary ideal MHD modes with low toroidal mode numbers ( $n=1,2,3$ ) are computed using the DCON code<sup>9</sup> to determine equilibrium stability. This code solves the Euler–Lagrange equation to minimize the potential energy and evaluates a real critical determinant whose poles indicate the presence of ideal instabilities. All MHD equilibria used herein were computed with the free boundary code CUBE.<sup>3</sup> The CUBE code utilizes a multigrid approach and a plasma current density constraint to obtain convergence at high Shafranov shift. A dozen external coils is uniformly distributed around the computational grid to constrain the plasma shape and position for any shift. These coils maintain a circular plasma cross section independent of the Shafranov shift. In this paper, we focus on low magnetic field plasma equilibria. After this introduction, we present a simple method which defines without any ambiguity highly shifted configurations. Next, we demonstrate the robustness of the stability of high  $\beta_p$  equilibria by scanning the current profile shapes and looking at the major source of instabilities. Finally, we show how the major parameters evolve as a stable path from low to high  $\beta_p$  equilibria is undertaken. In conclusion, we summarize our findings.

## II. A STRAIGHTFORWARD DEFINITION OF HIGH BETA POLOIDAL EQUILIBRIA

Since our study is based on the shape of the plasma toroidal current profile, it is useful to demonstrate how the toroidal current density actually constrains the plasma equilibrium. The physical model of the MHD equilibrium in the axisymmetric magnetic geometry of a tokamak is given by the Grad–Shafranov (GSh) equation,<sup>10</sup>

$$\Delta^* \psi = - \left( \mu_0 R^2 \frac{dp}{d\psi} + \frac{1}{2} \frac{dF^2}{d\psi} \right),$$

where

$$\Delta^* \psi \equiv R \frac{\partial}{\partial R} \left( \frac{1}{R} \frac{\partial \psi}{\partial R} \right) + \frac{\partial^2 \psi}{\partial Z^2} \quad (4)$$

in the usual toroidal coordinate system  $(R, Z, \phi)$ . We can also express Eq. (4) as a function of the toroidal current density flowing along the  $\phi$  direction,

$$\mu_0 J_\phi(R, \psi) = - \left( \mu_0 R \frac{dp}{d\psi} + \frac{1}{2R} \frac{dF^2}{d\psi} \right), \quad (5)$$

which yields

$$\Delta^* \psi = \mu_0 R J_\phi(R, \psi). \quad (6)$$

The quantity  $\psi$  is the flux of the poloidal magnetic field  $B_p$  in the  $(R, Z)$  plane,

$$\vec{B}_p = - \frac{1}{R} \frac{\partial \psi}{\partial Z} \vec{e}_R + \frac{1}{R} \frac{\partial \psi}{\partial R} \vec{e}_Z, \quad (7)$$

and the function  $F$  represents the net poloidal current flowing through a disk centered on the  $Z$ -axis and located on the  $(R, \phi)$  plane,<sup>11</sup>

$$F = B_\phi R. \quad (8)$$

Equations (4) and (6) describe the local equilibrium between the gradient of the fluid pressure  $p$  and the Lorentz force. Usually,  $p$  increases monotonically from the plasma–vacuum interface to the magnetic axis,<sup>11</sup> where it reaches a maximum. It can be demonstrated that the pressure  $p$  and the toroidal function  $F$  are functions of  $\psi$  only. Thus, the surfaces of constant pressure correspond to surfaces of constant flux. The flux  $\psi$  always varies monotonically from the plasma edge to the magnetic axis. Since the GSh equation has two different forms, either can be used, depending on how one wishes to solve the problem at hand. The standard form, Eq. (4), has two free functions,  $p$  and  $F$ ; the other form, Eq. (6), has only one free function  $J_\phi(R, Z)$ . Since the toroidal current profile is the principal factor driving the Shafranov shift, due to flux conservation on both sides of the magnetic axis, we propose to define  $p$  and  $F$  as a function of  $J_\phi(R, Z)$ , instead of the more common method, which uses  $p$  and  $F$  directly. Since these functions depend on  $\psi$  only, they are completely defined only if  $J_\phi(R, Z)$  is given along a path that encompasses the whole range of  $\psi$ . If this path stretches from one edge of the plasma to the other, via the magnetic axis, this condition is satisfied. A natural approach consists of using the current profile on the plasma midplane, i.e.,  $J_\phi(R, Z_{\text{axis}})$ , where  $Z_{\text{axis}}$  is the vertical location of the mag-

netic axis. When solving the GSh equation numerically, we can divide the toroidal current profile into two distinct current profiles located on each side of the magnetic axis. The profile on the high field side (HFS) of the axis is called  $J_{\phi\text{HFS}}$ , and the profile on the low field side (LFS)  $J_{\phi\text{LFS}}$ . Using Eq. (5) only, we find on the same flux surface that

$$\frac{dp}{d\psi} = \frac{R_{\text{LFS}}J_{\phi\text{LFS}}(R_{\text{LFS}}, Z_{\text{axis}}) - R_{\text{HFS}}J_{\phi\text{HFS}}(R_{\text{HFS}}, Z_{\text{axis}})}{R_{\text{LFS}}^2 - R_{\text{HFS}}^2} \quad (9)$$

and

$$\frac{dF^2}{d\psi} = 2\mu_0 R_{\text{LFS}}R_{\text{HFS}} \times \frac{R_{\text{LFS}}J_{\phi\text{HFS}}(R_{\text{HFS}}, Z_{\text{axis}}) - R_{\text{HFS}}J_{\phi\text{LFS}}(R_{\text{LFS}}, Z_{\text{axis}})}{R_{\text{LFS}}^2 - R_{\text{HFS}}^2}. \quad (10)$$

$R_{\text{LFS}}, R_{\text{HFS}}$  is the radial location on the  $Z=Z_{\text{axis}}$  plane where  $J_{\phi}$  is equal to  $J_{\phi\text{LFS}}(R_{\text{LFS}}, Z_{\text{axis}})$ ,  $J_{\phi\text{HFS}}(R_{\text{HFS}}, Z_{\text{axis}})$ , respectively. In this procedure,  $p$  and  $F$  are always defined as long as  $\psi$  is monotonic. Once  $p$  and  $F$  are computed, the numerical solution of the GSh equation proceeds in the conventional manner. However transforming the GSh equation into a single parameter equation governed only by  $J_{\phi}(R, Z_{\text{axis}})$  greatly simplifies the definition of highly shifted configurations since the location of the magnetic axis is only dependent on the shape of the current profile.<sup>3</sup> Furthermore, the toroidal current profile distribution is generically geometric, facilitating its connection to the plasma equilibrium.

Equation (9) raises an important point. To obtain high plasma pressures  $dp/d\psi$  has to be as positive as possible. As a consequence,  $J_{\phi\text{LFS}}$  has to be large compared to  $J_{\phi\text{HFS}}$ . This also entails that the plasma has to be diamagnetic, since  $dF^2/d\psi$  is negative in this case. It now becomes straightforward to construct any high pressure equilibria by simply setting  $J_{\phi}$  to zero on the HFS portion of the toroidal current profile, as suggested by Cowley.<sup>12</sup> This leads to high  $\beta_p$  configurations (also called asymptotic configurations<sup>12</sup>) where the magnetic axis is located near the low field side edge of the plasma. When a shift of the magnetic axis occurs, the toroidal current density  $J$  can be increased significantly before the minimum value of the safety factor  $q$  drops below 1. While large toroidal currents still confine the pressure gradient on the outboard side of the plasma, the rest of the pressure is confined by the poloidal currents running in the remainder of the plasma cross section. Thus, for the same confining magnetic field, high  $\beta_p$  devices can confine higher pressures than their low  $\beta_p$  counterparts, as illustrated by Fig. 1(b). The Shafranov shift alters not only the shape of the flux surfaces but also the current density distribution. After constructing a high beta equilibrium and solving numerically the GSh equation using the toroidal plasma current profile as a code input, it becomes straightforward to study the stability of such equilibria as a function of the shape of the current profiles.

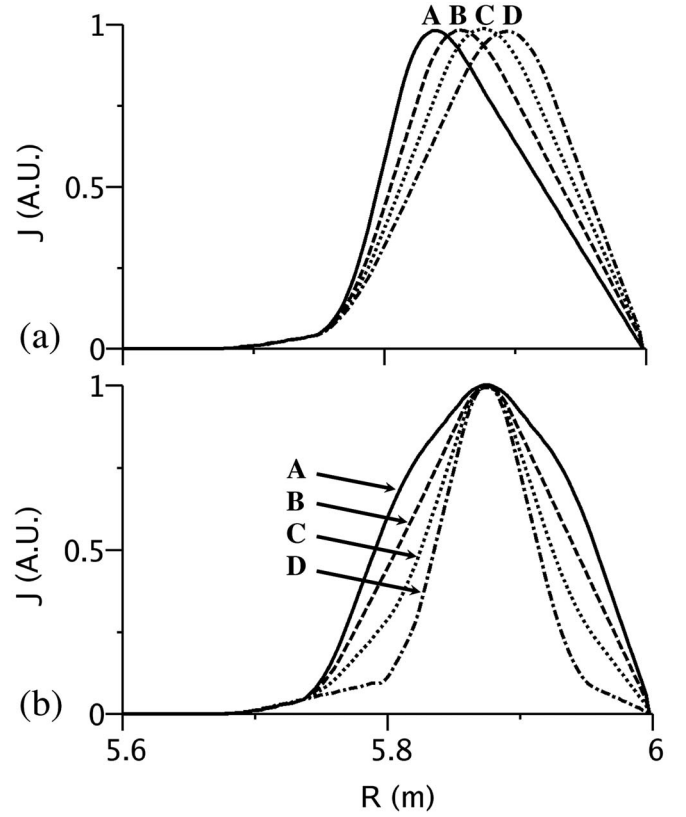


FIG. 2. Current profile scans used in the stability study of high  $\beta_p$  equilibria. (a) Peak position and (b) peaking factor scans. The plasma extends from  $R=4$  m to  $R=6$  m. Part of the null region of the current profile has been truncated from the plots to enlarge the section where shape changes occur. The magnetic axis is located around  $R=5.80$  m.

### III. THE STABILITY OF HIGH BETA POLOIDAL EQUILIBRIA

In this section, we examine the relationship between current profile shape and plasma stability. The equilibria presented herein are stable to all internal modes with toroidal numbers  $n=1,2,3$  as well as being Mercier stable.<sup>4</sup> By changing the shape of the current profile we try to simulate the degree of inaccuracy that a real experiment may encounter when using feedback control on the shape of the current profile. First we will study the evolution of the stability as the peak of the current profile is being moved along the radial direction. Then we will investigate the impact of the current profile width on instabilities.

As the location of the current peak with respect to the magnetic axis changes, instabilities occur. The resulting shape modifications are indicated in Fig. 2(a). Profile A has a central  $q$  just below 1. This is the limit to the current peak scan since safety factors smaller than 1 are usually unstable. As the peak moves to the low field side of the plasma,  $\beta$  decreases while the whole  $q$  profile rises. Figure 3(a) shows the different criteria as a function of the normalized radius,  $\rho=r/a$ . In this parameter scan, the only concern lies with local GGJ resistive instabilities which emerge as the peak of the profile moves away from the magnetic axis. The high- $n$  ballooning criterion is never violated in this scan. In fact, the peak location does not alter this criterion in a meaningful

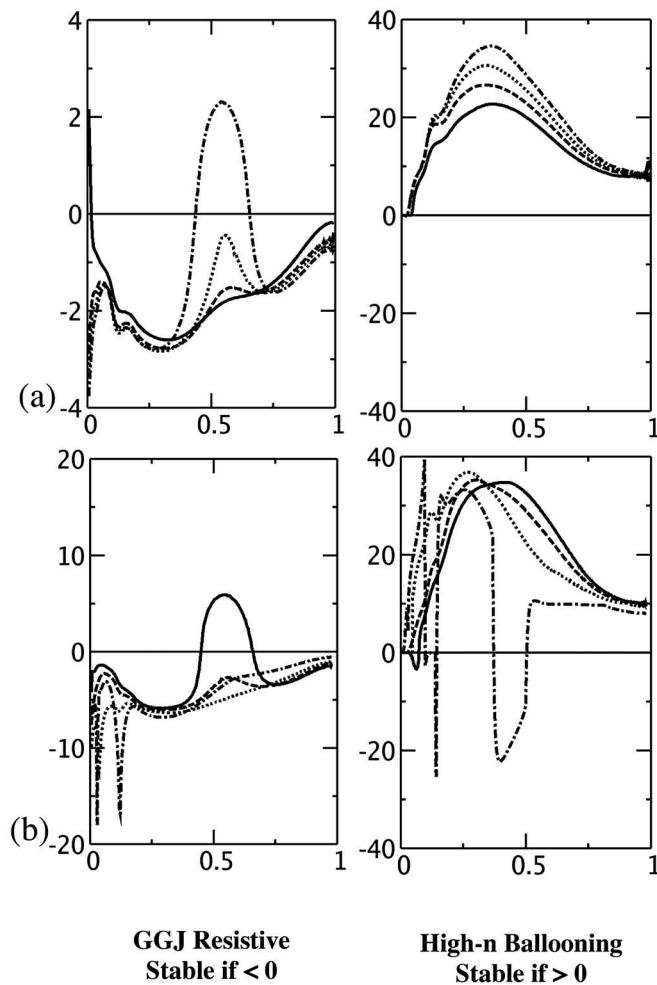


FIG. 3. GGJ resistive and high- $n$  ideal ballooning criteria of profiles A (solid lines), B (dashed lines), C (dashed-dotted lines), and D (dotted lines) for (a) peak location and (b) peaking factor scans. The different criteria are plotted as a function of  $\rho(=r/a)$ ;  $\rho=0$  is at the magnetic axis and  $\rho=1$  at the plasma edge. The ordinates of all curves are in arbitrary absolute units. In the left column, the part of the profiles that is positive shows instabilities to resistive interchange instabilities. In the right column, the profiles are stable if the criterion is positive.

manner. We observe that relatively large swings of the current profile peak are not likely to push the equilibrium into an unstable regime of operation. All profiles bounded by profiles B and C are stable to GGJ instabilities and high- $n$  ballooning modes. The safety margin on the GGJ criterion between stable and unstable regions is sufficiently large to insure robust stability across the entire profile. The change in peak position barely affects the Shafranov shift.

The different profiles investigated in the scans of the current peak width are collected in Fig. 2(b). Profile D is particularly interesting because the strong peaking in current density significantly increases the pressure that can be confined. The width of the current density peak influences the pressure and  $q$  profiles only in a region surrounding the magnetic axis. The stability results for this scan are collected in Fig. 3(b). Current profile A is hampered by high- $n$  ballooning instabilities. Broad profiles such as profile D are impervious to ballooning modes. However they are infested by resistive interchange instabilities in a large region of the plasma.

Broad profiles also lower the effective plasma pressure, which makes them even less attractive. Profiles B and C have acceptable stability properties and should be sought in experiments. Furthermore, profile C was found to be stable to free boundary modes with  $n=1, 2$ , and 3.

While the current shape was modified in a noticeable manner, no instabilities were detected for the “central” profiles B and C, allowing a degree of flexibility on the current profile shape on the order of 10%. During these current scans, all fixed boundary modes with toroidal mode numbers 1, 2 or 3 were found stable. On the other hand, free boundary modes remain a serious issue since they are often unstable. While this can be an impediment to highly shifted equilibria, they can be stabilized to a certain extent using toroidal rotation and resistive wall mode feedback.<sup>13</sup> It is reasonable to assume that as stabilization techniques evolve, such equilibria can be sustained. Since all finite aspect ratio tokamaks start at low  $\beta_p$ , such an outcome is interesting only if we can find at least one stable path from low to high  $\beta_p$ . The next section explores such a path.

#### IV. PLASMA EVOLUTION TO HIGH BETA POLOIDAL

To characterize the evolution of the plasma parameters with  $\beta_p$ , one can start from a stable low  $\beta_p$  configuration, and carefully evolve the current profile, keeping all the major MHD criteria in check, to obtain higher  $\beta_p$  configurations. A smooth transition between the current profiles presented herein could very well yield a continuous path to high pressure plasmas. Our strategy has incorporated two important approaches. First, we require that the profiles be evolved contiguously. Second, if the change in one shaping parameter leads to instabilities, then the evolution was continued using a different shaping parameter until other instabilities were encountered. The systematic repetition of this process yielded a stable path from our initial low- $\beta_p$  equilibrium to a high  $\beta_p$  equilibrium, the evolution of which at no point crosses into an unstable region of parameter space. By stable, we mean here stable to the MHD criteria enumerated earlier except for external modes.

The variety of allowable current shapes is rather dependent on the Shafranov shift. While relative freedom exists at high shifts ( $\sim 50\%$  or more), stable configurations at intermediate Shafranov shifts ( $\sim 20\% - 40\%$ ) are more difficult to find. It was also necessary to insure that the margins of allowable variation for each case overlapped with adjacent cases, guaranteeing that the path is truly contiguous. All  $q$  profiles have everywhere-positive shear, as the reduction in magnetic shear may trigger high- $n$  ballooning modes.<sup>14</sup> Because the plasma current is constant, the value of  $q$  on axis stays in the unity range. The minimum plasma current for which  $q_{\min}$  stays above 1 for the duration of the transition is  $I_p=50$  kA. Starting from the classical pyramidal shape of low beta plasmas, Fig. 4(a) shows the progression of the current profile to 40% Shafranov shift. The reader should note that the current profiles used herein were voluntarily presented in Fig. 4 as straight broken lines in a spirit of simplicity. However the stability study was done using smooth current profiles. It is also important to mention that

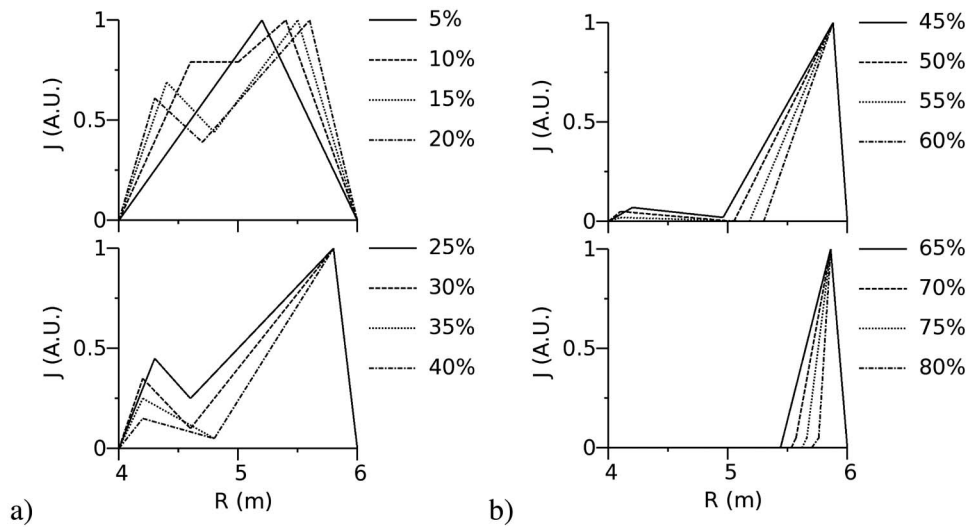


FIG. 4. Stable high beta path from 5% to 80% shift. The current profile shapes presented here are simplified by using a series of broken lines. The current profiles studied are smooth. The degree of smoothness of the current does not modify the stability.

current profile smoothing, when not extreme, does not fundamentally change the DCON stability results. The off-axis current peak appearing on the high field side of the plasma is necessary to keep the local magnetic shear strictly positive throughout the transition. The current plateau at the 10% mark is necessary so that a smooth transition can occur between the pyramidal to the double pyramidal current shape. As the current peak shifts to the low field side, the high field side pyramid can be reduced progressively. From 20% to 25% both the high field side shoulder of the current and peak location continue to move synchronously. Beyond the 25% mark, the strong current gradient on the low field side of the plasma is kept constant as the high field side current density is reduced. This keeps the adequate nonreversing  $q$  profile while increasing the Shafranov shift. At the 40% mark, both peak location and high field side current peak are altered simultaneously. Figure 4(b) shows that once the optimal low field side current gradient has been found (45% shift) it needs little adjustment throughout the rest of the transition. Only the high field side structure sustains large alterations. Passing the 60% shift mark,  $q$  profiles with positive shear do not require any currents on the high field side. This feature can be completely suppressed and only the main current peak remains. As the current is compressed on the low field side of the plasma, the sharp transition between the null current density region and the strong gradient region has to be adjusted slightly to avoid further instabilities.

As the plasma  $\beta_p$  becomes large, it is instructive to examine the evolution of some physical plasma parameters. The plasma poloidal and peak betas increase with Shafranov shift. Figure 5(a) shows the steady rise of all betas, except for  $\beta_N$ . As the shift reaches our 80% target, the region of high pressure reduces and concentrates around the magnetic axis. As  $\beta$  increases, a  $\beta_N$  saturation just below 6 occurs. Sustaining  $\beta_N$  of 6 remains an open question but it seems possible experimentally by extending and improving existing control techniques.<sup>13</sup> Since we wish to keep the plasma cross section constant, elongation effects were not studied herein. However, one should note that elongated shapes tend to reduce the value of  $\beta_N$ . It is important to remark that, for the

same plasma current, there is an order of magnitude enhancement in peak  $\beta$  compared to a low shift configuration.

Because we maintain positive magnetic shear,  $q$  increases from the magnetic axis to the edge. Figure 5(b) shows the central and edge  $q$  evolution as the magnetic axis moves to the low field side of the plasma. Below a shift of 25%, the central  $q$  increases while the edge  $q$  remains constant. As the shift increases, the central  $q$  decays until it reaches 1 for a shift of 80%. Meanwhile, the edge  $q$  increases rapidly. Above shifts of about 60%, an interesting phenomenon occurs. The central  $q$  saturates slightly above 1 while the edge  $q$  continues to increase at a constant rate, indicating that the global shear increases with the shift. This favors stronger magnetic shear which tends to stabilize ballooning modes. This large difference between  $q_{\min}$  and  $q_{\max}$  points to the presence of strong poloidal diamagnetic currents, digging the well in the toroidal magnetic field. Figure 5(c) shows the toroidal function differential ( $F_{\text{axis}} - F_{\text{edge}}$ ). The well is clearly visible with a reduction of 10% of the toroidal magnetic field on axis. Moreover, Fig. 5(c) illustrates the substantial increase in pressure as the axis approaches the low field side.

## V. SUMMARY

We presented in this paper the stability of highly shifted tokamak equilibria. First we used a straightforward definition of high  $\beta_p$  plasmas based on the toroidal current density alone. This definition guarantees large shifts by simply forcing the high field side current density to zero. We then showed that equilibria can be varied over a wide range of parameters while remaining stable to the Mercier and high- $n$  ballooning instabilities, as well as fixed boundary modes for  $n=1, 2$ , and 3. Furthermore we have presented the theoretical existence of a stable path to high  $\beta_p$  configurations for a finite aspect ratio low-field tokamak. Starting from a typical low  $\beta_p$  equilibrium, a series of incremental changes in the current profile distribution have transformed a low pressure equilibrium into a high  $\beta_p$  configuration. Detailed control of the current profile is necessary to perform the manipulations

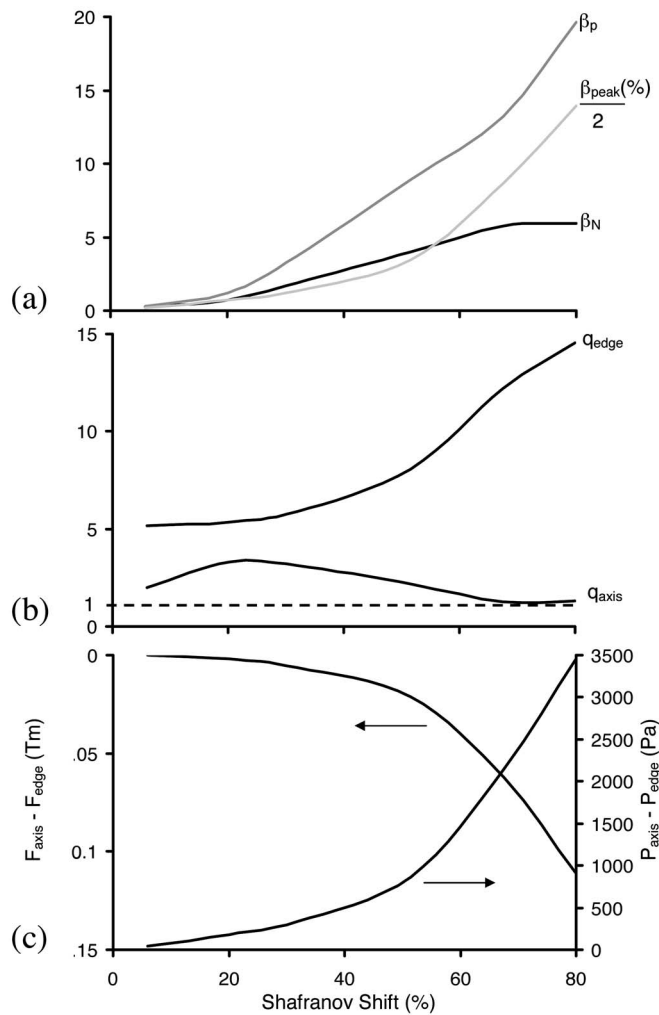


FIG. 5. (a) Poloidal, peak, and normal betas; (b) central and edge  $q$  values; and (c) pressure and toroidal function differentials as a function of Shafranov shift.

required for the transition, as well as keeping the highly shifted configurations stable. With larger outward shifts of the magnetic axis, there is a steady increase in peak  $\beta$ . We observed saturation of the central  $q$  and  $\beta_N$ , and the rapid formation of a magnetic well. The experimental feasibility of such a path is not yet established since current profile modifications could lead to potentially unstable equilibria. However its existence, by itself, represents an important piece of information. High  $\beta_p$  equilibria could be reached from their low  $\beta_p$  counterparts, especially without encountering high- $n$  ballooning modes, a major confinement issue when going to higher plasma pressures. More penalizing than stability is the experimental run time. If any stable path can be found, the significant (controlled) modifications of the current profile proposed in this paper should be envisaged on the resistive time scale. Many present day machines cannot run long enough to allow the diffusion of the plasma current. On the other hand, this should not be an issue for a reactor which should operate continuously and with bootstrap currents, providing a large portion of the high  $\beta_p$  current distribution presented in Fig. 4(b). Furthermore the evolution of the plasma parameters along this path is quite revealing. One

unexpected result comes from the saturation in  $\beta_N$ . Indeed, high  $\beta_p$  equilibria can have relatively low  $\beta_N$ .

The reader will note that other common (ideal or resistive) MHD instabilities such as free boundary, medium- $n$  or tearing modes also need to be investigated to further study MHD stability. While this paper does not close the subject on MHD stability, it does show that high  $\beta_p$  configurations are stable to some of the most common MHD instabilities, such as the internal kink modes or Mercier instabilities. Since these instabilities do not theoretically develop in high  $\beta_p$  configurations, other sources of instabilities can become dominant and it remains vital to understand the underlying problems posed by such equilibria on all levels of MHD stability, ideal or resistive. However this work opens the door to new research directions where high plasma pressure would not be as limiting as previously thought. In fact, many negative phenomena at low  $\beta_p$  tend to disappear at high  $\beta_p$ . We mention here that the connection length, which is the distance along the field lines from the outboard midplane to the plasma core, is shorter at high  $\beta_p$ . This provides some stability to ballooning and microinstabilities. This also yields that the volume in the bad curvature region is small so the average curvature is very good. Furthermore, the presence of the magnetic well is an important factor that positively affects microstability.<sup>15</sup> The magnetic well reverses the trapped particle drifts. As a consequence, it takes energy to remove a trapped particle from the well (preserving their adiabatic invariants) thereby enhancing microstability. Overall, this work indicates that high  $\beta_p$  configurations should be considered anew as a serious candidate for fusion energy production.

## ACKNOWLEDGMENTS

This paper was supported by the U.S. DOE under Grant Nos. DE-FG02-04ER54740 (NCTE) and DE-FG02-04ER54737.

- <sup>1</sup>F. Troyon, R. Gruber, H. Saurenmann, S. Semenzato, and S. Succi, *Plasma Phys. Controlled Fusion* **26**, 209 (1984).
- <sup>2</sup>P.-A. Gourdain and J. N. Leboeuf, *Phys. Plasmas* **11**, 4372 (2004).
- <sup>3</sup>P.-A. Gourdain, J. N. Leboeuf, and R. Y. Neches, *J. Comput. Phys.* **216**, 275 (2006).
- <sup>4</sup>P.-A. Gourdain, S. C. Cowley, J.-N. Leboeuf, and R. Y. Neches, *Phys. Rev. Lett.* **97**, 055003 (2006).
- <sup>5</sup>R. J. Taylor, J.-L. Gauvreau, M. Gilmore, P.-A. Gourdain, D. J. LaFontaine, and L. W. Schmitz, *Nucl. Fusion* **42**, 46 (2002).
- <sup>6</sup>C. Mercier, *Nucl. Fusion* **1**, 47 (1960).
- <sup>7</sup>A. H. Glasser, J. M. Greene, and J. L. Johnson, *Phys. Fluids* **18**, 875 (1975).
- <sup>8</sup>J. W. Connor, R. J. Hastie, and J. B. Taylor, *Phys. Rev. Lett.* **40**, 396 (1978).
- <sup>9</sup>A. H. Glasser and M. S. Chance, *Bull. Am. Phys. Soc.* **42**, 1848 (1997).
- <sup>10</sup>V. D. Shafranov, *Reviews of Plasma Physics* (Consultants Bureau, New York, 1966), Vol. 2, pp. 103–151.
- <sup>11</sup>J. P. Freidberg, *Ideal Magnetohydrodynamics* (Plenum, New York, 1987).
- <sup>12</sup>S. C. Cowley, P. K. Kaw, R. S. Kelly, and R. M. Kulsrud, *Phys. Fluids B* **3**, 2066 (1991).
- <sup>13</sup>E. J. Strait, J. Bialek, N. Bogatu, M. Chance, M. S. Chu, D. Edgell, A. M. Garofalo, G. L. Jackson, T. H. Jensen, L. C. Johnson, J. S. Kim, R. J. LaHaye, G. Navratil, M. Okabayashi, H. Reimerdes, J. T. Scoville, A. D. Turnbull, M. L. Walker, and the DIII-D Team, *Nucl. Fusion* **43**, 430 (2003).
- <sup>14</sup>J. W. Connor and R. J. Hastie, *Phys. Rev. Lett.* **92**, 075001 (2004).
- <sup>15</sup>C. Bourdelle, W. Dorlan, X. Garbet, G. W. Hammett, M. Kotschenreuther, G. Rewoldt, and E. J. Synakowski, *Phys. Plasmas* **10**, 2881 (2003).